Supporting Information

Construction of aqueous supercapacitors with oxidation suppression of nickel phosphide via interfacial engineering and electric field modulation for enhanced secondary energy storage

Haiyang Zhai, Jie He*, Suili Shi, Mingtang Liu, Zhibing Wang, Zhiliang Jin*

School of Chemistry and Chemical Engineering, Ningxia Key Laboratory of Solar Chemical Conversion Technology, Key Laboratory for Chemical Engineering and Technology, State Ethnic Affairs Commission, North Minzu University, Yinchuan 750021, P.R.China

Corresponding author: 2014138@nun.edu.cn (J. He); zl-jin@nun.edu.cn (Z. L. Jin).

Results and discussion

1. Crystallographic, morphological, and elemental composition

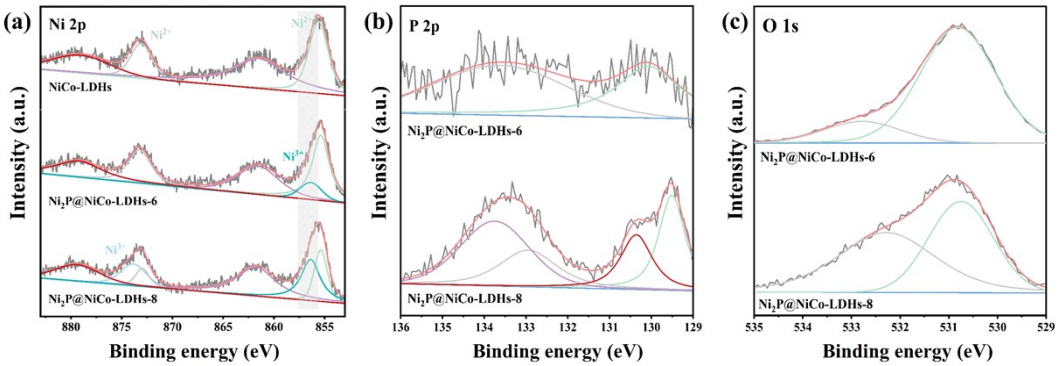

Figure S1. XPS analysis and mapping: **(a)** Ni 2p; **(b)** P 2p; **(c)** O 1s.

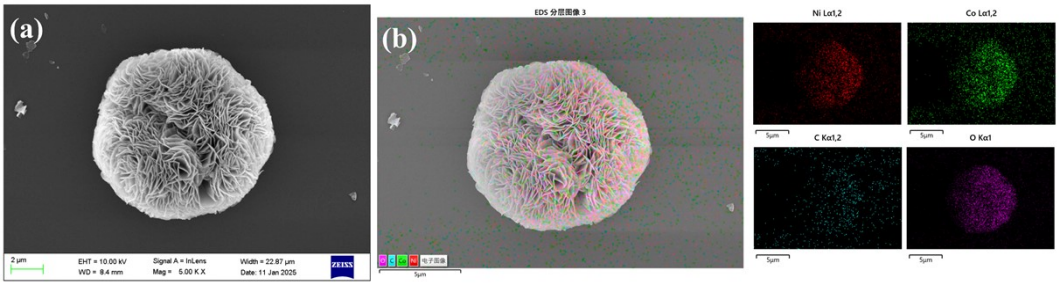

Figure S2. **(a)** and **(b)** Elemental mapping graphs of nickel-cobalt hydrotalcite.

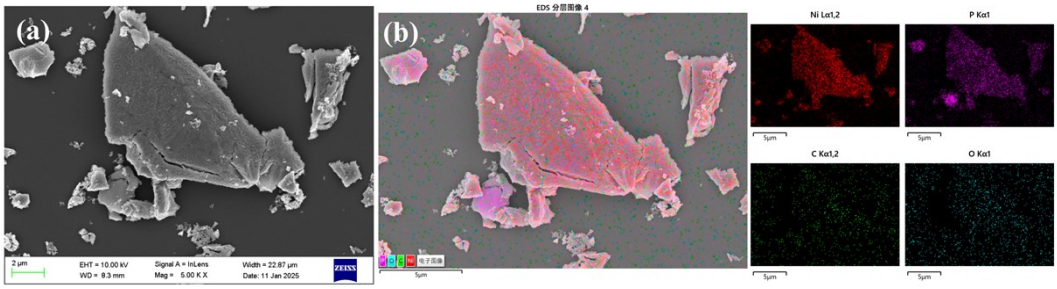

Figure S3. **(a)** and **(b)** Elemental mapping graphs of Ni_2P.

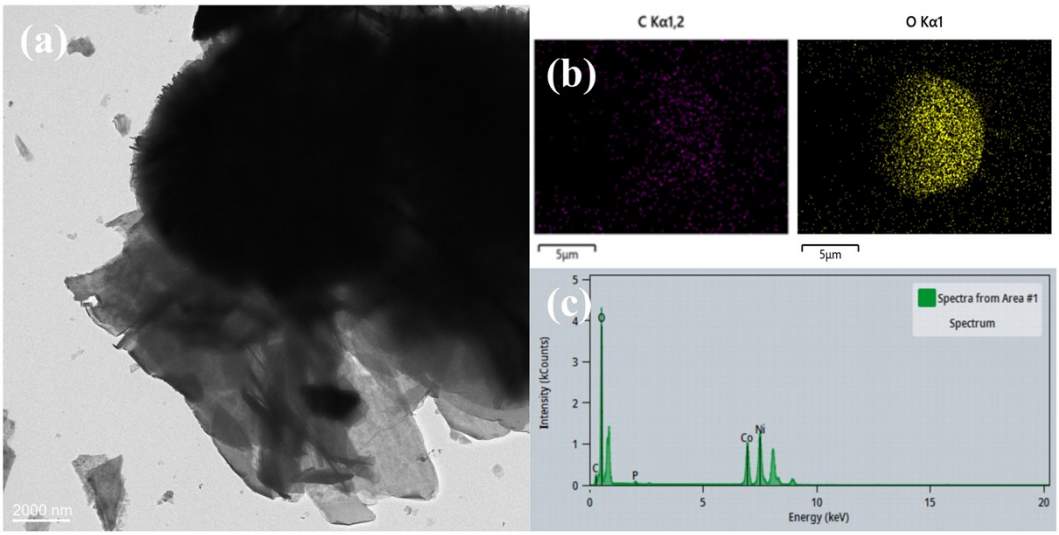

Figure S4. (a) Low-magnification morphologies of Ni_2P@NiCo-LDHs-6; **(b)** Elemental mapping graphs of Ni_2P@NiCo-LDHs-6; **(c)** Elemental content diagram of Ni_2P@NiCo-LDHs-6.

2. First principle calculations

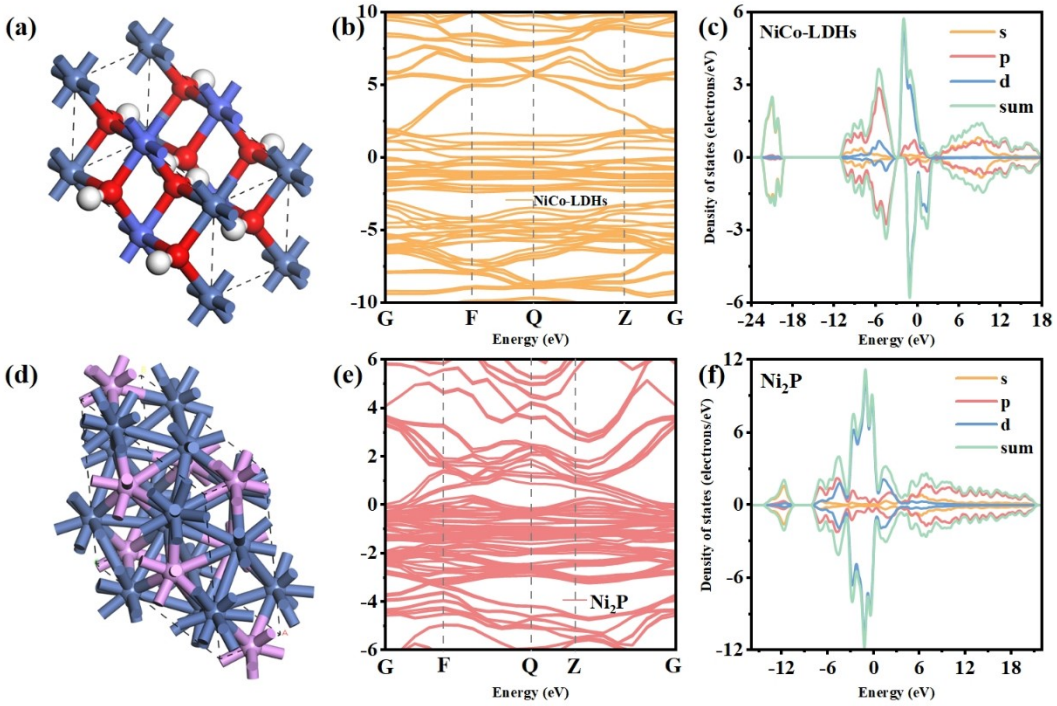

Figure S5. The following were calculated for nickel cobalt layered double hydroxide and nickel phosphide: **(a)** and **(d)** structural models; **(b)** and **(e)** energy level diagrams; **(c)** and **(f)** density of states diagrams.

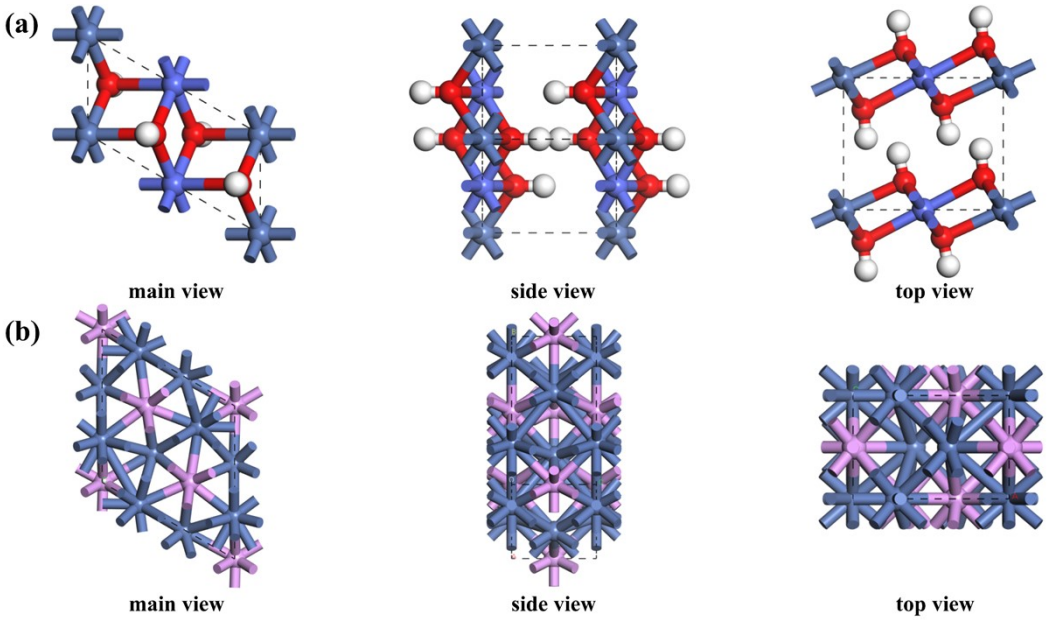

Figure S6. **(a)** Three-view diagrams of the nickel cobalt hydrotalcite model; **(b)** Three-view diagrams of the nickel phosphide model.

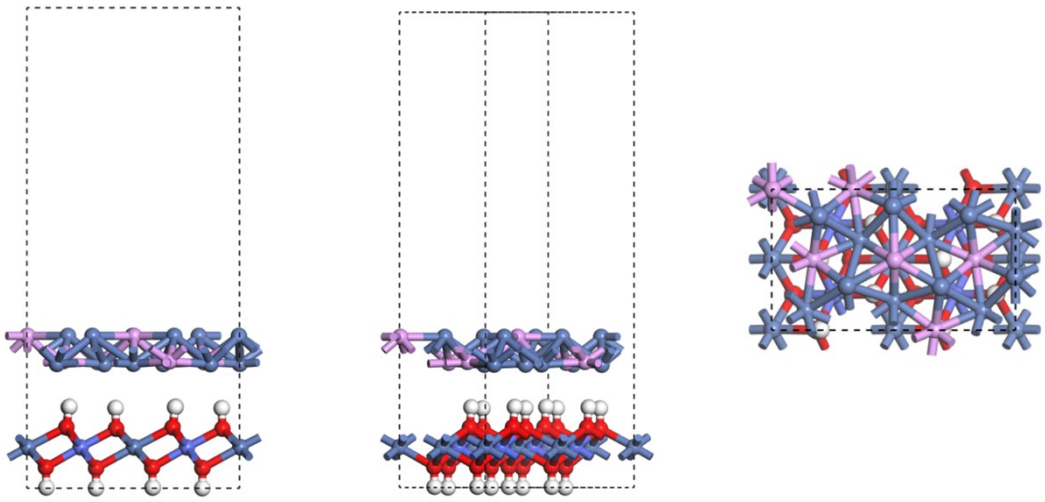

Figure S7. Three-view diagrams of the constructed Ni_2P@NiCo-LDHs heterostructure model.

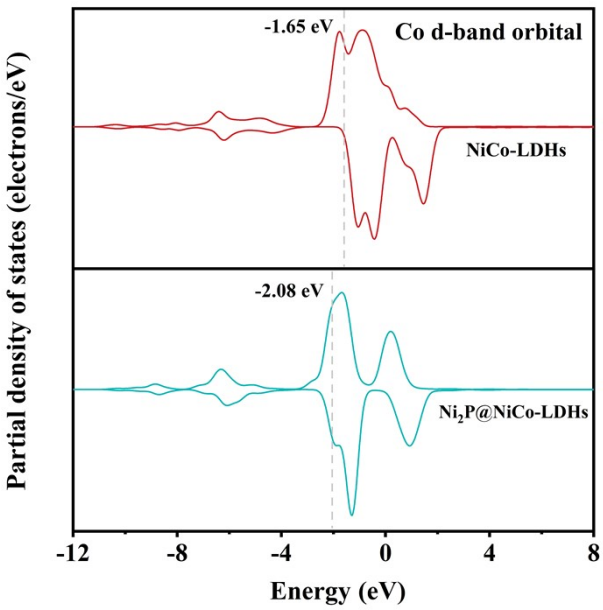

Figure S8. The d-orbital center of Co in the calculated Ni_2P@NiCo-LDHs heterostructure model.

3. Three-Electrode System

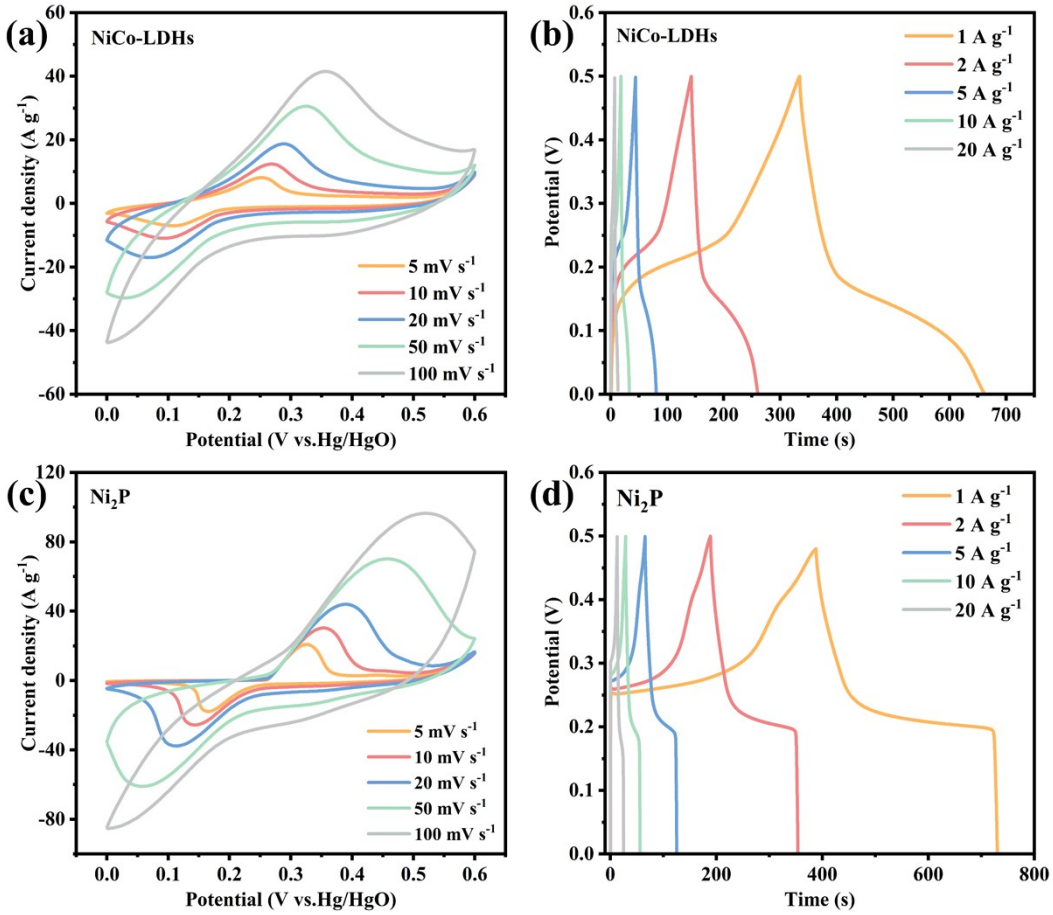

Figure S9. (a) CV curve of NiCo-LDHs; **(b)** GCD curve of NiCo-LDHs; **(c)** CV curve of Ni_2P; **(d)** GCD curve of Ni_2P.

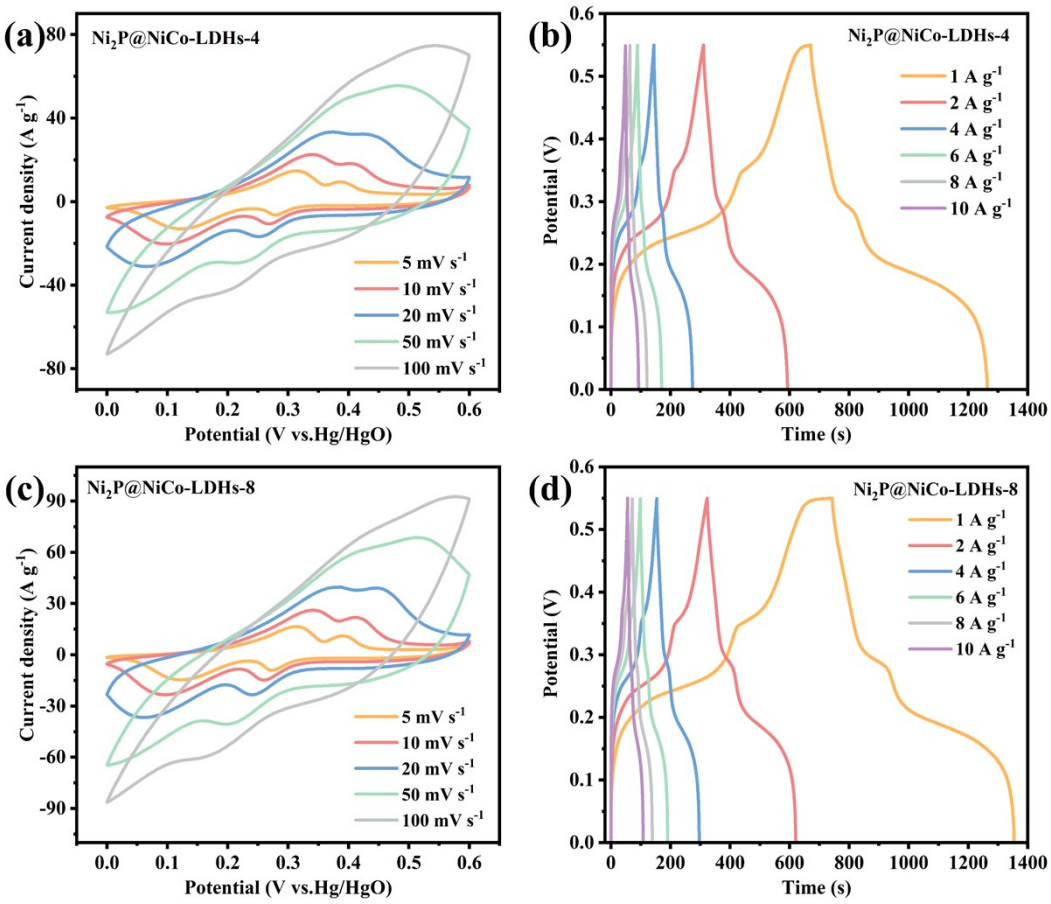

Figure S10. (a) CV curve of Ni_2P@NiCo-LDHs-4; **(b)** GCD curve of Ni_2P@NiCo-LDHs-4; **(c)** CV curve of Ni_2P@NiCo-LDHs-8; **(d)** GCD curve of Ni_2P@NiCo-LDHs-8.

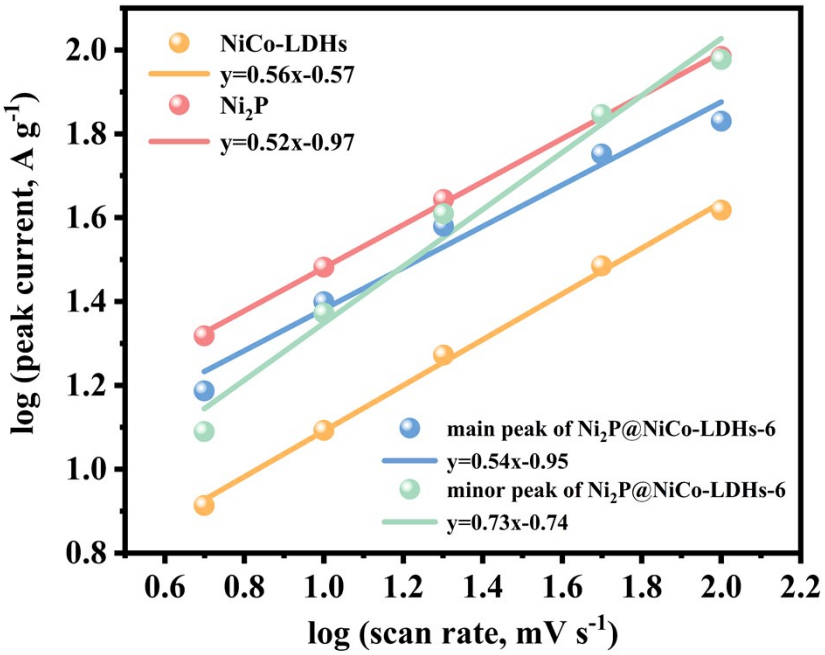

Figure S11. The relationship between the logarithm of the peak-to-peak current of anodes composed of different materials and the logarithm of the scan rate.

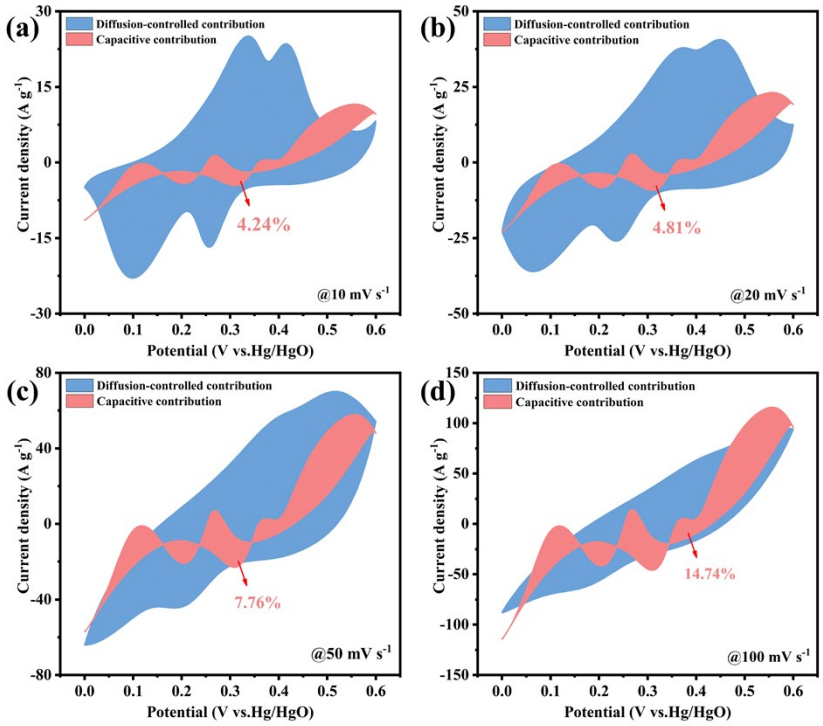

Figure S12. The proportion of the double-layer capacitance control to the total capacitance control at different scanning rates in Ni_2P@NiCo-LDHs-6.

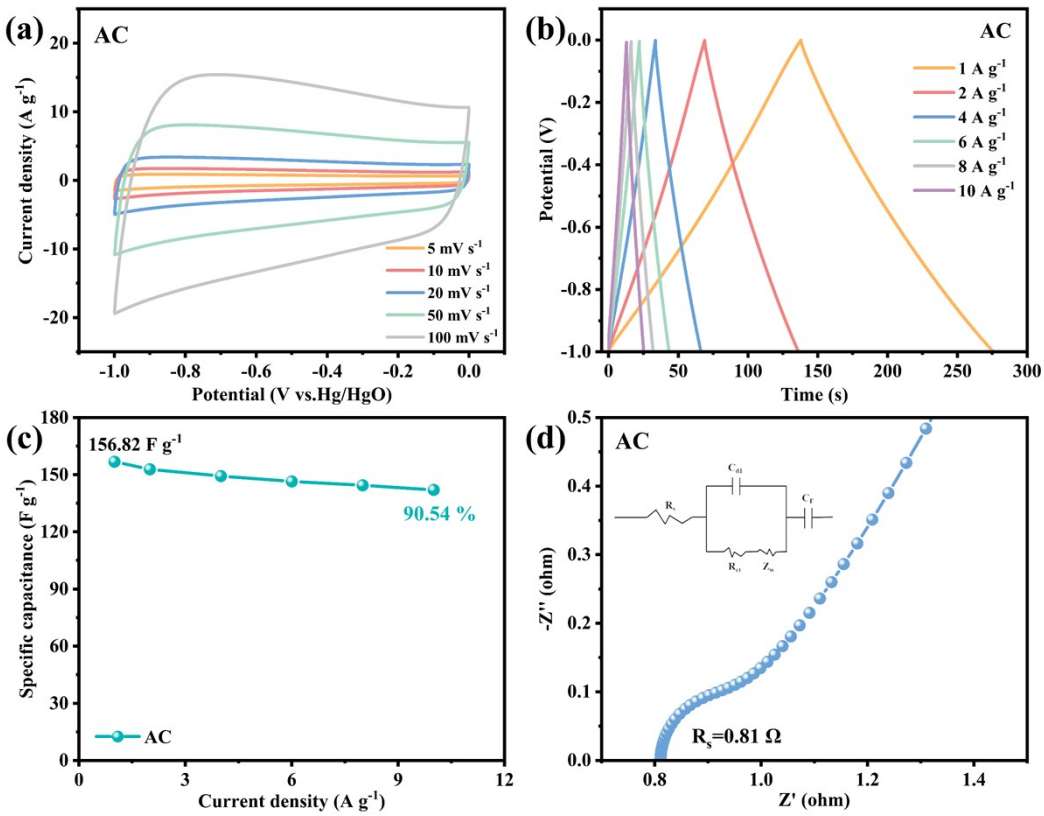

Figure S13. The following of AC materials employed in the assembly of asymmetric supercapacitors: **(a)** CV curves; **(b)** GCD curves; **(c)** specific capacitance and capacitance retention rate; **(d)** EIS curves.

Table S1. Electrochemical performance comparison of electrode materials in this work with previously published works.

Electrode materials	Specific capacitance	Rate capability	Capacitance retention	Reference
Ni_2P@NiCo-LDHs	1001.46 F g^{-1} at 1 A g^{-1}	75.63% at 10 A g^{-1}	92.86% after 4000 cycles	This work
NiCo MOF-2	927.1 F g^{-1} at 1 A g^{-1}	69.7% at 10 A g^{-1}	-	1
NiCoS/ACC	413.3 F g^{-1} at 1 A g^{-1}	78.39% at 5 A g^{-1}	86% after 5000 cycles	2
MXene-LDH	983.98 F g^{-1} at 2 A g^{-1}	54.53% at 50 A g^{-1}	76% after 5000 cycles	3
NiCo/NMCS-50	585 F g^{-1} at 1 A g^{-1}	36.6% at 10 A g^{-1}	-	4
CoS_x/NiCo LDH	1903.8 F g^{-1} at 1 A g^{-1}	76.1% at 10 A g^{-1}	-	5
NiCo/NHCS-23	536 F g^{-1} at 1 A g^{-1}	64.7% at 10 A g^{-1}	-	6
NiCo LDHMs/NF-100	1156 F g^{-1} at 1 A g^{-1}	72% at 10 A g^{-1}	95.37% after 5000 cycles	7
MO/NMO/NiCo LDH	815 F g^{-1} at 1 A g^{-1}	23.72% at 20 A g^{-1}	-	8
Ni-Co-S-10	640 F g^{-1} at 1 A g^{-1}	-	84% after 10000 cycles	9
NiCoP/HMCS-2	856.06 F g^{-1} at 1 A g^{-1}	87.07% at 20 A g^{-1}	86.45% after 5000 cycles	10

Table S2. the Nyquist impedance value of the electrode in the three electrodes.

Electrode	Mass content (mg)	R_{ct} (Ω)
Ni_2P	1.7	3.78
NiCo-LDHs	1.56	0.67
Ni_2P@NiCo-LDHs-4	1.63	0.24
Ni_2P@NiCo-LDHs-6	1.61	0.21
Ni_2P@NiCo-LDHs-8	1.68	0.22

Table S3. Energy density for the Ni_2P@NiCo-LDHs-6//AC ASC device with other ASC devices reported preciously. The reference numbers are consistent with the main text.

Electrode materials	Power density (W kg^{-1})	Energy density (W h kg^{-1})	Ref.
$Ni_2P/NiSe_2/MoSe_2$//AC	400	23.5	67
NiP/NCHTs//AC	1125	46.53	68
NiCo-LDH@$Ni(OH)_2$//AC	799.9	30.6	69
Mo-Ni_2P/Co2P//AC	800	35.56	70
$WS_2/NiCo(PO_4)_3$/MXenes//AC	703	38	71
NiCo-LDH/Ni/CC//AC	750	49.3	72
Ni_2P/CNT//AC	749.8	25.2	73
Ni_2P@NiCo-LDHs-6//AC	766.81	51.88	This work

Table S4. the Nyquist impedance values of assembled asymmetric supercapacitors.

Asymmetric supercapacitors	**R_{ct} (Ω) 5,500 cycles before**	**R_{ct} (Ω) 5,500 cycles after**
Ni_2P//AC	0.47	5.84
Ni_2P@NiCo-LDHs-6//AC	0.25	2.14

References

[1] Yongquan Du, Ruibin Liang, Junxi Wu, Yingyi Ye, Shaoyong Chen, Jian Yuan, Jianwen Chen, Peng Xiao, High-performance quasi-solid-state flexible supercapacitors based on a flower-like NiCo metal-organic framework, ***RSC Advances*****,** 2022, 12, 5910-5918.

[2] Shaofei Zhang, Jing Ren, Tao Gu, Hao Guo, Hongquan Wang, Muhammad Imran, Rui-Peng Ren, Yong-Kang Lv, Porous NiCoS nanosheets decorated activated carbon cloth for flexible asymmetric supercapacitors, ***Diamond and Related Materials*****,** 2022, 127, 109154.

[3] H. Li, F. Musharavati, E. Zalenezhad, X. Chen, K. N. Hui, K. S. Hui, Electrodeposited NiCo layered double hydroxides on titanium carbide as a binder-free electrode for supercapacitors, ***Electrochimica Acta*****,** 2018, 261, 178-187.

[4] Raju Ranjithkumar, Ji Ho Youk, Nitrogen-doped mesoporous carbon spheres decorated with NiCo alloy nanoparticles for high-performance electrochemical supercapacitors, ***Journal of Electroanalytical Chemistry*****,** 2024, 960, 118183.

[5] Fujuan Luo, Yisong Wang, Lei Han, Kai Tao, Amorphous/Crystalline CoS_x/NiCo Layered Double Hydroxide Nanosheet Arrays for Asymmetric Supercapacitors, ***ACS Applied Nano Materials*****,** 2025, 8, 4179-4187.

[6] Raju Ranjithkumar, Ji Ho Youk, Nitrogen-doped hollow carbon spheres decorated with NiCo alloy nanoparticles for high-performance supercapacitor electrode, ***Materials Today Chemistry*****,** 2024, 36, 101939.

[7] Shanshan Bai, Bingzhe Jia, Yuxuan Zhang, Huailin Yang, Xinrui Qiang, Xinming Wu, Mitigating self-discharge in supercapacitors through strategic mesoporous structural modification of NiCo layered double hydroxides, ***Journal of Alloys and Compounds*****,** 2024, 1002, 175441.

[8] Ruibin Liang, Si Liu, Jianrong Lin, Jingfei Dai, Jingyi Peng, Peiyuan Huang, Jianwen Chen, Peng Xiao, A high mass loading flexible electrode with a sheet-like Mn_3O_4/$NiMoO_4$@NiCo LDH on a carbon cloth for supercapacitors, ***RSC Advances*****,** 2023, 13, 33463-33470.

[9] Yuxiang Wen, Yanpeng Liu, Ting Wang, Zilei Wang, Yanan Zhang, Xiaogang Wu; Xueting Chen; Shanglong Peng; Deyan He, High-Mass-Loading Ni–Co–S Electrodes with Unfading Electrochemical Performance for Supercapacitors, ***ACS Applied Energy Materials*****,** 2021, 4, 6531-6541.

[10] Shuling Liu, Jiaru Fan, Lei Ren, Qiangqiang Shi, Yue Wang, Jiale Guo, Jianbo Tong, Nickel–Cobalt Bimetallic Phosphide/Hollow-Structured Carbon Nanosphere Composites for Supercapacitor Electrode Materials, ***ACS Applied Nano Materials*****,** 2024, 7, 25628-25636.